

Design and Development of Mathematical Equivalent Circuit Model of Broadband Circularly Polarized Semi-Annular Ring-Shaped Monopole Antenna

Priya R. Meher* and Sanjeev K. Mishra

Abstract—This article presents a broadband circularly polarized (CP) semi-annular ring-shaped printed monopole antenna for wireless applications. A semi-annular monopole with symmetric partial ground plane is designed to achieve the impedance bandwidth with a behaviour of linearly polarized (LP) radiation wave. To achieve the CP behaviour with broadband axial ratio (AR) bandwidth, an asymmetric stair-shaped partial ground plane is incorporated in the semi-annular ring-shaped monopole structure. Different analysis of CP radiation is presented by analysing the surface current distribution, electric field distribution, and also its mathematical modelling using CST-MWS solver. Moreover, an equivalent circuit model of the proposed monopole antenna is developed using Foster canonical forms. The measured -10 dB impedance bandwidth and 3-dB AR bandwidth are 8.78 GHz [3.22–12.0 GHz] and 2.21 GHz [7.58–9.79 GHz], respectively. The peak realized gain and antenna efficiency are 4.32 dB at 7.61 GHz and 82% at 4.83 GHz, respectively. The proposed antenna can be suitable for C-band (4–8 GHz) and X-band (8–12 GHz) applications.

1. INTRODUCTION

Due to the requirement of more than one application in a single system, printed monopole antennas have been introduced rapidly from the last two decades onwards. They are popularly used because of their striking advantages like low profile, ease of fabrication, broad impedance bandwidth, omnidirectional radiation pattern, good time-domain performance, and ease of integration with RF circuits [1–4]. In literature, many research works are based on LP monopole antennas [5–8] which provide multipath signal reception and misalignment of the antenna that causes polarization mismatch losses. To overcome these losses, CP printed monopole antennas have been introduced. In the present scenario, CP monopole antenna plays a significant role in modern wireless communication systems because it offers independent antenna orientation between Tx & Rx, and less multipath distortion, etc. than LP antennas. The concept behind the CP antenna is to generate two orthogonal electric field vectors with a 90° phase difference, and their corresponding amplitude remains the same. In literature, CP is achieved by introducing parasitic elements or strips on a partial ground plane with a printed monopole antenna like a dual spiral parasitic strip [9] that obtains 2.2 GHz AR bandwidth. Similarly, the rectangular parasitic element [10] along with I-slot on the partial ground plane is for generating dual AR bandwidths of 0.7 GHz and 0.25 GHz, respectively. Furthermore, feeding technique [11] is also responsible for generating CP radiation wave. Besides, some of the CP techniques related to modifying the physical geometry of printed monopole or introducing an asymmetric ground plane such as Y-shaped monopole [12], rectangular-hexagonal slot with L-shaped monopole [13], asymmetric partial ground

Received 9 December 2022, Accepted 11 January 2023, Scheduled 26 January 2023

* Corresponding author: Priya Ranjan Meher (c117008@iiit-bh.ac.in).

The authors are with the Department of Electronics and Telecommunication Engineering, International Institute of Information Technology Bhubaneswar, Odisha, India.

plane [14], and G-shaped parasitic with C-shaped monopole [15] also generate dual orthogonal electric field vectors with 90° time-phase difference, achieving CP. However, their mathematical modelling of CP and equivalent circuit model of monopole is still unexplored.

In this article, a semi-annular ring-shaped monopole antenna with stair shaped asymmetric partial ground plane in frequency domain (F-D) analysis as well as time domain (T-D) analysis is proposed for wireless application. By placing an asymmetric stair-shaped partial ground plane along with a semi-annular printed monopole, a broadband CP with broader impedance bandwidth is achieved. To realize the CP, different methodologies like surface current distribution and electric field distribution with their mathematical modeling are investigated using CST-MWS solver. Furthermore, the equivalent circuit model is developed using Foster canonical forms.

2. ANTENNA CONFIGURATION

Figure 1 shows the schematic diagram of the proposed semi-annular ring-shaped monopole antenna with stair-shaped asymmetric partial ground plane antenna. It is fed by a $50\text{-}\Omega$ microstrip transmission line printed on an FR-4 epoxy substrate.

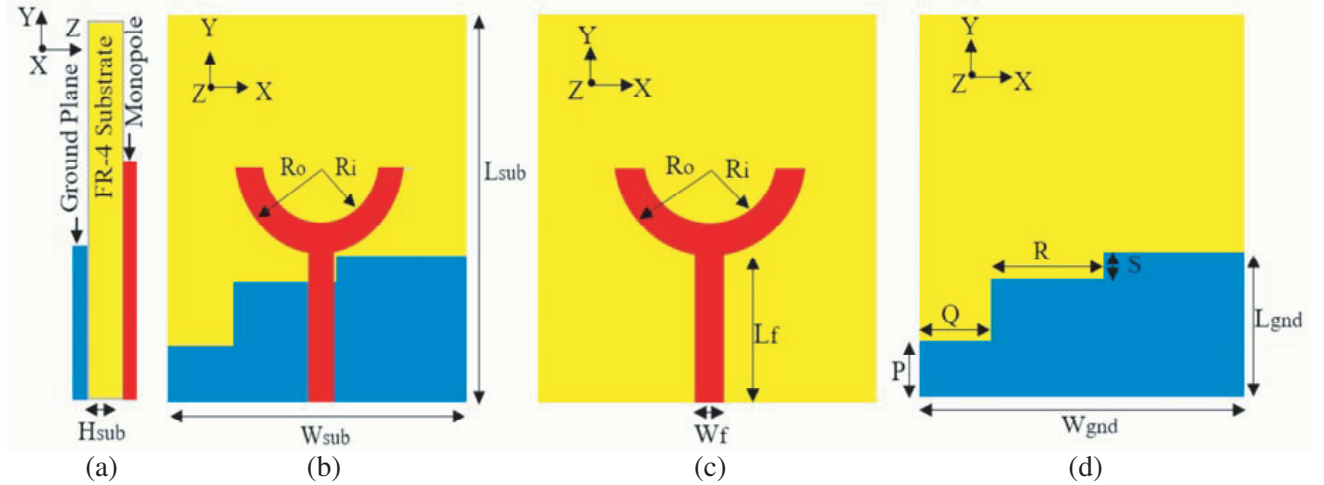


Figure 1. Geometry of the proposed antenna. (a) Side view. (b) Front view with ground plane. (c) Top view. (d) Bottom view. [Optimized dimensions: $L_{sub} = 47$, $W_{sub} = W_{gnd} = 46$, $L_{gnd} = 15$, $H_{sub} = 1.6$, $R_o = 9.7$, $R_i = 7$, $L_f = 15$, $W_f = 2.7$, $P = 5.8$, $Q = 10.1$, $R = 15$ and $S = 2.7$. All dimensions are in mm].

The semi-annular monopole is printed on the substrate, and it acts as a radiator. Similarly, an asymmetric stair-shaped partial ground plane is printed below the substrate. The proposed structure is designed and analyzed using CST-MWS and HFSS softwares.

2.1. Evolution of Semi-Annular Monopole Antenna

Figure 2 shows the evolution of printed semi-annular monopole antenna. The proposed structure is transformed from a circular monopole into a semi-annular radiator. Initially, circular monopole with symmetric partial ground plane is designed and their radius (R_o) is calculated [16] by using the following Equation (1):

$$R_o = \frac{7.2 - gF_L}{2.25F_L} \quad (1)$$

where g is the separation between radiating monopole and partial ground plane, and F_L is the lower resonant frequency of the circular monopole structure. From the simulated point of view, the current is highly dense at the edge part of the circular monopole rather than a central part of the circular monopole structure. Therefore, the central part of the monopole structure is removed, resulting in an

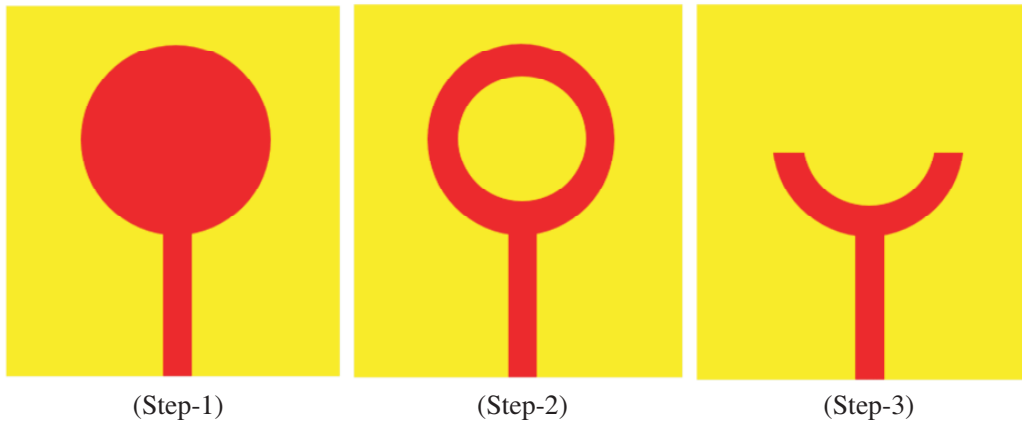


Figure 2. Evolution of semi-annular ring-shaped monopole antenna.

annular ring-shaped monopole antenna, and it generates TM_{11} mode within the operating frequency band. It is also verified theoretically as well as simulated in CST solver. Theoretically, the resonant frequency (f_{res}) for the TM_{11} mode of annular ring-shaped monopole antenna [17] is calculated by the following Equation (2):

$$f_{res, TM_{11}} = \frac{2C_0}{6.283 \times (R_o + R_i) \times \sqrt{\epsilon_{reff,sub}}} \tag{2}$$

where, $\epsilon_{reff,sub} = \frac{1}{2}(\epsilon_{r,sub} + 1) + \frac{1}{2}(\epsilon_{r,sub} - 1) \left(1 + \frac{H_{sub}}{R_o - R_i}\right)^{-\frac{1}{2}}$

C_0 is the velocity of EM wave in free space; R_o & R_i are the outer and inner radius of the printed semi-annular monopole; $\epsilon_{r,sub}$ & $\epsilon_{reff,sub}$ are the permittivity & effective permittivity of the substrate; and H_{sub} is the height of the substrate. The calculated and simulated resonant frequencies are 3.12 and 3.08 GHz, respectively, and their corresponding mode is observed as shown in Fig. 3(b). In order to make the semi-annular monopole structure, the upper part of annular-shape is removed, and as a result, the resonant frequency gets shifted from 3.08 GHz to 3.48 GHz with an enhancement of impedance bandwidth. The reason behind the shifting of resonant frequency and the enhancement of impedance bandwidth is the decrease in the equivalent inductance of the antenna.

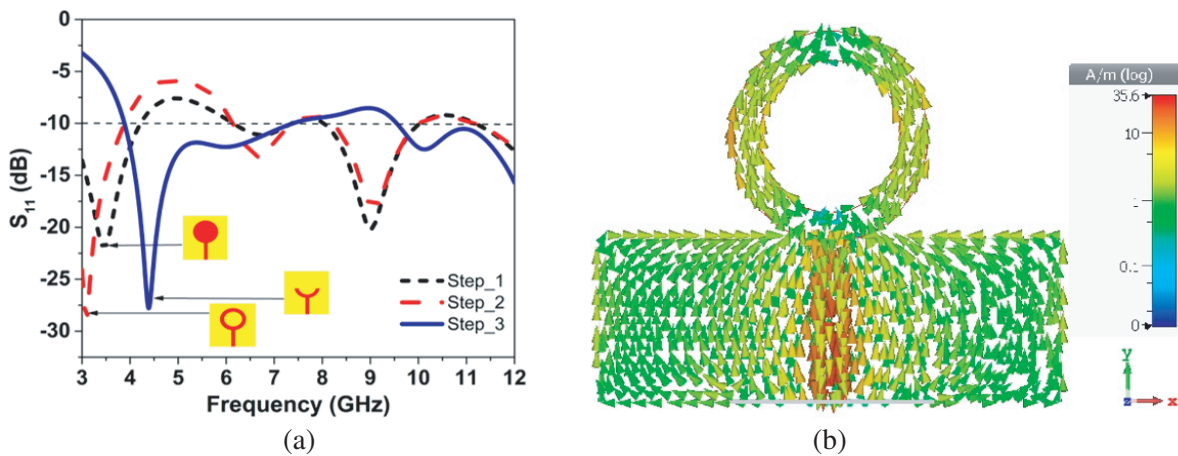


Figure 3. Output responses of the monopole antenna. (a) S_{11} characteristics. (b) Surface current distribution at 3.08 GHz.

2.2. Evolution of Asymmetric Partial Ground Plane

Figure 4 shows the evolution of an asymmetric partial ground plane embedded with a semi-annular shape printed monopole radiator. Initially, a symmetric partial ground plane with a semi-annular printed monopole radiator (Stage-1), i.e., similar to Fig. 3(a) (Step_3), is designed that provides LP waves, and its corresponding AR plot belongs to the 40 dB line. In order to transform LP into CP waves, some part of the partial ground plane is perturbed, i.e., stage-2, and its corresponding AR plot gets shifted downward up to 7 dB. Similarly, again perturbing the other part of the partial ground plane, i.e., stage-3, provides CP radiation waves, and its corresponding AR curve belongs to below 3 dB line as shown in Fig. 5.

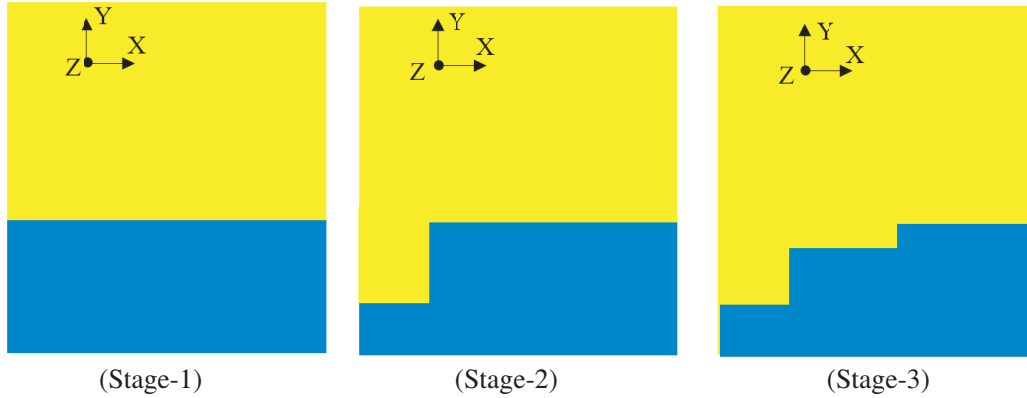


Figure 4. Evolution of asymmetric partial ground plane.

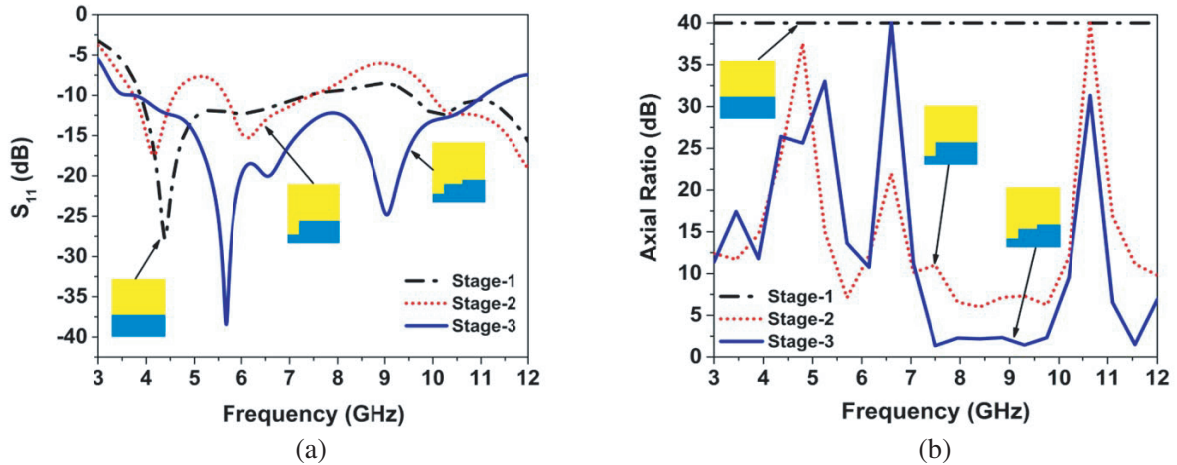


Figure 5. Output responses of different stages asymmetric ground plane. (a) S_{11} characteristic. (b) AR characteristics.

3. PARAMETRIC STUDY AND CP MECHANISM

3.1. Parametric Study

This section presents the effects of stair-shaped partial ground plane parameters like stair-shaped lengths P , S , and width R on impedance bandwidth and AR bandwidth vs frequency. With the help of antenna parameter analysis, the researcher can choose the optimized dimension of different parameters of the proposed antenna. Initially, the length of a partial ground plane (L_{gnd}) is optimized with different

values, which indicates the gap between radiating semi-annular monopole and a stair-shaped partial ground plane. The optimized value is 15 mm. Here, the capacitance that results from the corner gap between the partial ground plane and radiating monopole logically balances the inductance of the proposed antenna [16].

Figure 6 shows the effect on S_{11} and AR by varying the stair-shaped length P . The variation of length has more effect on CP radiation waves. The optimized value is 5.8 mm, at which it provides a better result in terms of S_{11} & AR bandwidth. Fig. 7 shows S_{11} and AR characteristics by varying the stair-shaped width R . The proposed antenna provides better performance at $R = 15$ mm. Similarly, Fig. 8 illustrates the effect of different values of S on S_{11} and AR bandwidth. Here, both results play a major role in choosing the optimized value of the length because a small variation can affect antenna outcome results. The optimized value of S for getting better performance is 2.7 mm.

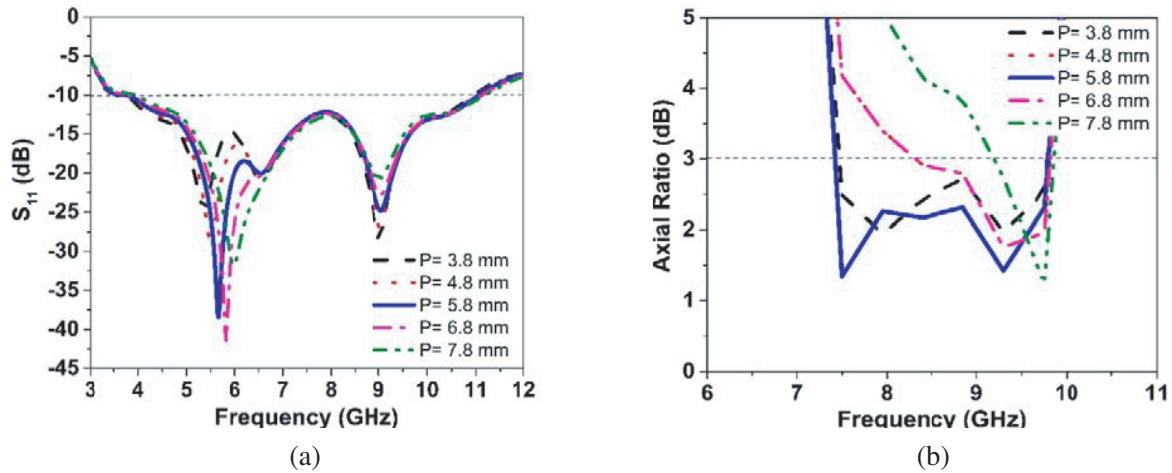


Figure 6. Simulated results at different P values. (a) S_{11} characteristics. (b) AR characteristics.

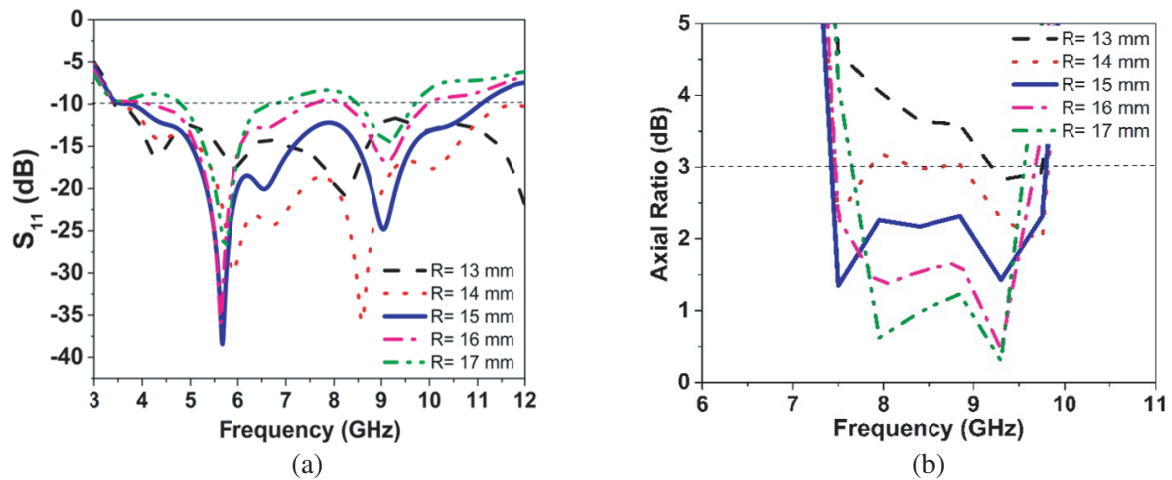


Figure 7. Simulated results at different R values. (a) S_{11} characteristics. (b) AR characteristics.

3.2. CP Mechanism

In general, the printed monopole antenna with a symmetric partial ground plane provides linear polarization which may be either horizontally or vertically polarized. Fig. 9(a) shows the surface current distribution for a symmetric ground plane with LP monopole antenna at 4.4 GHz. The proposed

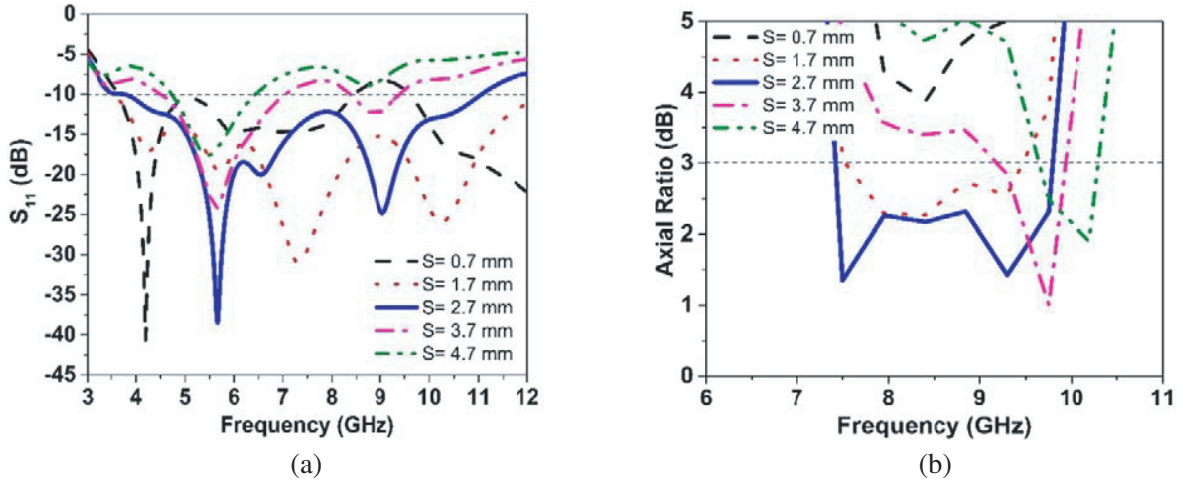


Figure 8. Simulated results at different S values. (a) S_{11} characteristics. (b) AR characteristics.

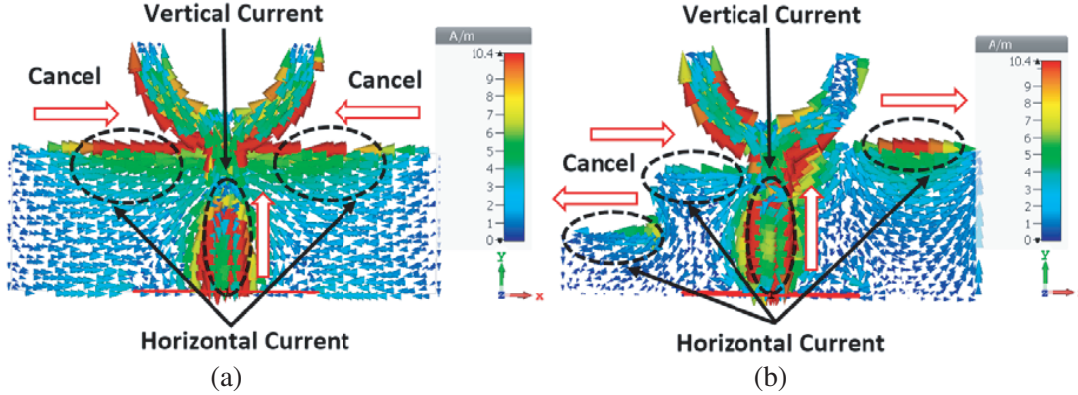


Figure 9. The surface current distribution of the proposed antenna. (a) Symmetric ground plane at 4.4 GHz. (b) Asymmetric ground plane at 7.9 GHz.

structure generates both horizontal as well as vertical currents, but horizontal currents on the partial ground plane are opposite to each other, i.e., 180° phase difference with the same magnitude. Thus, the horizontal components on the ground plane cancel each other, and it provides very weak radiation in horizontal rather than vertical direction at far-field radiation.

To achieve CP radiation, a part of the partial ground plane is perturbed, and an asymmetric stair-shaped partial ground plane is formed which generates both horizontal and vertical currents, but some parts of horizontal currents are cancelled to each other due to 180° phase difference. Finally, there is a presence of horizontal as well as vertical currents, which leads to CP radiation waves as shown in Fig. 9(b). For better understanding CP, the surface current distribution on the ground plane for different phases, i.e., 0° , 90° , 180° , and 270° at 7.9 GHz are illustrated in Fig. 10. It is observed that the time-varying surface current distributions at 0° and 180° are equal in magnitude but opposite in phase. Similarly, the same behaviour is observed at 90° and 270° [18, 19]. It indicates that the proposed monopole antenna is right-handed circularly polarized (RHCP) in the far-field region.

Furthermore, to validate the CP radiation, electric field (E-field) distributions are investigated using CST-MWS software. The mathematical equations of the E-fields [20, 21] are expressed in Equations (3)–(4).

The total E-fields can be written as:

$$E(z, t) = (E_{xo}e^{j\omega t}\hat{x} + E_{yo}e^{j\omega t}\hat{y}) e^{-j\beta z} \quad (3)$$

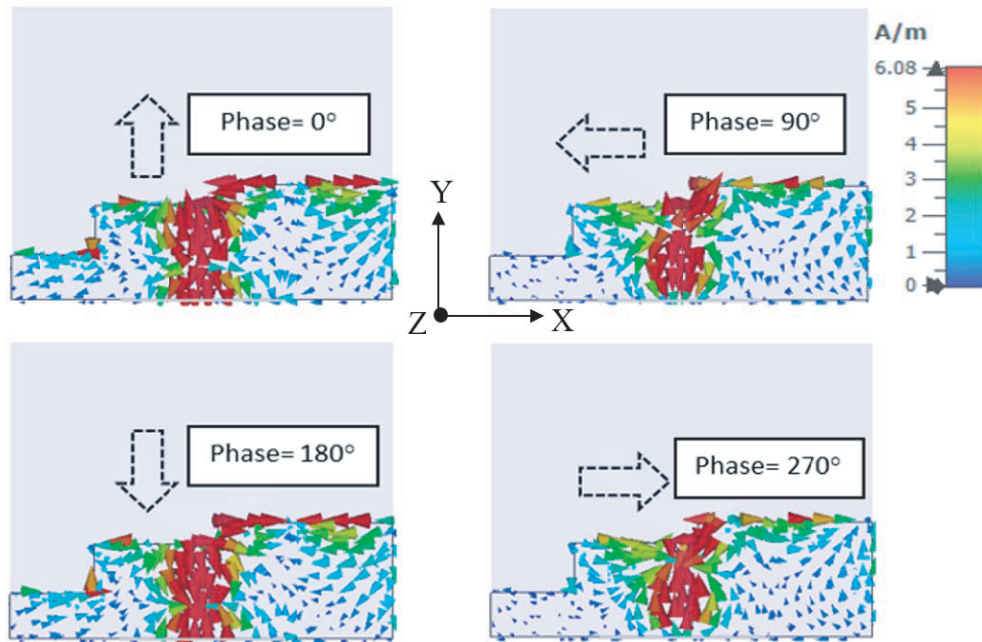


Figure 10. The surface current distribution on ground plane at 7.9 GHz.

The condition for CP, $E_{x_0} = E_{y_0} = E_0$ (Equal Amplitude) and $E_{x_0} = E_0 e^{j0}$ & $E_{y_0} = E_0 e^{j\frac{\pi}{2}}$ (Difference Phase). At $z = 0$ (propagation of the electromagnetic wave), the resultant equation will be:

$$E(0, t) = E_0 \cos(\omega t) \hat{x} + E_0 \cos\left(\omega t + \frac{\pi}{2}\right) \hat{y} \tag{4}$$

By implementing the different phases values in Equation (4), the graphical representations of x and y components of E-fields are presented in Table 1. When the phase is shifted from 0° to 90° , the orientations of E-fields are also changed from horizontal (+ve) to vertical (+ve) directions that confirm the formation of orthogonal modes [21]. Hence, the proposed structure generates CP. For phase angles 0° , 90° , 180° , and 270° , the rotation of E-field is a counterclockwise motion to the direction of propagation along the z -axis [22, 23]. Thus, the designed antenna is also called as RHCP monopole antenna.

Table 1. Orientation of field at different phases in the proposed structure.

Phase (ωt)	$E_0 \cos(\omega t)$	$E_0 \cos(\omega t + 90^\circ)$	Implimentation of theory in proposed structure for different phases at 7.9 GHz
0°	E_0	0	
90°	0	$-E_0$	
180°	$-E_0$	0	
270°	0	E_0	

4. EQUIVALENT CIRCUIT OF THE PROPOSED MONOPOLE ANTENNA

In general, the behaviour of antennas is linear that consists of passive elements resonating at multiple frequencies [24]. It is represented by Foster canonical forms as shown in Fig. 11. The 1st Foster canonical form is applicable to the modelling of electric antennas such as dipole and monopole antennas that behave as an open circuit at DC input signal as shown in equation [25] (5).

$$Z_{in} = j \left(\omega L_0 - \frac{1}{\omega C_0} \right) + \sum_{n=1}^N \left(\frac{\omega^2 L_n^2 R_n}{(R_n - \omega^2 L_n R_n C_n)^2 + \omega^2 L_n^2} + j \frac{\omega R_n^2 L_n (1 - \omega^2 L_n C_n)}{(R_n - \omega^2 L_n R_n C_n)^2 + \omega^2 L_n^2} \right) \quad (5)$$

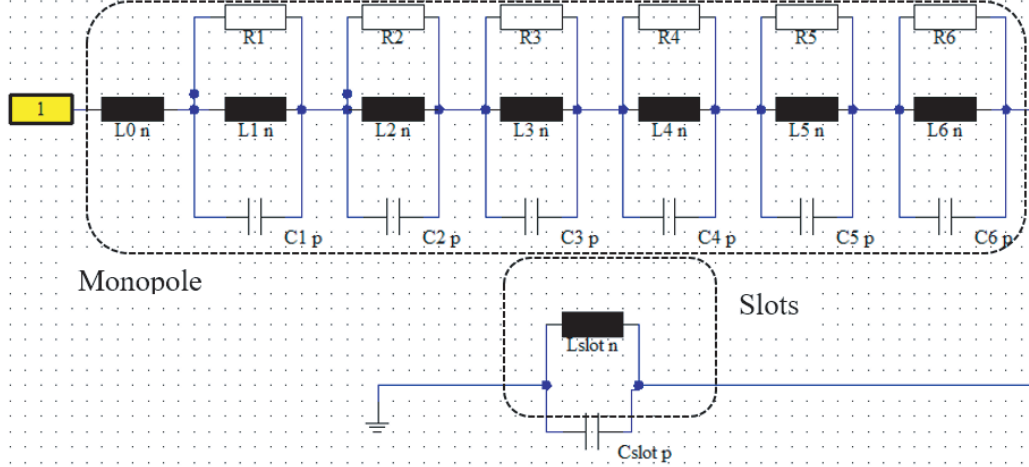


Figure 11. Equivalent circuit diagram of the proposed monopole antenna.

Similarly, the 2nd Foster canonical form is applicable to the modelling of magnetic antennas such as loop antennas that behave as electrically short at DC input signal. In the case of proposed monopole antenna, the equivalent circuit model consists of series resistor and capacitor with a series of parallel R-L-C tanks for different resonating modes. Furthermore, the stair-shaped ground plane is presented along with a monopole antenna. So, the slots are taken into account, i.e., series of parallel C_{slots} and L_{slots} with complete circuits. The equivalent circuit diagram is shown in Fig. 11.

Here, series capacitor acts as a static capacitor that arises due to printed patch and the ground plane, as the monopole antenna is devoid of ground plane below the patch. Thus, the series capacitor is neglected. Therefore, single inductor in series and series of parallel R-L-C tanks with series of parallel C_{slots} and L_{slots} are adequate to represent the proposed monopole antenna.

The return loss and its corresponding real and imaginary parts of impedance are shown in Figs. 12(a) and (b), respectively. The total number of resonators of the proposed monopole antenna depends on the number of zeros crossing in the imaginary part of the impedance graph. It is observed from the impedance graph, the total number of zeros crossing is six, i.e., (1)–(6). The value of real part of the impedance is obtained from the impedance plot. The different values of the resistance (R_{in}) and reactance, i.e., inductance (L_n) and capacitance (C_n), corresponding to proposed monopole antenna with slots are reported in Table 2.

Table 2. Lumped element value of the proposed monopole antenna.

Z_{in}	Z_0	Z_1	Z_2	Z_3	Z_4	Z_5	Z_6	Z_{slot}
R_{in} (Ω)		130.94	39.2	47.7	53.73	27.8	57.1	
L_n (nH)	0.1	2.14	1.24	2.74	0.1	0.1	5.98	1
C_n (pF)		3.24	0.1	10.22	2.29	6.34	3.24	0.1

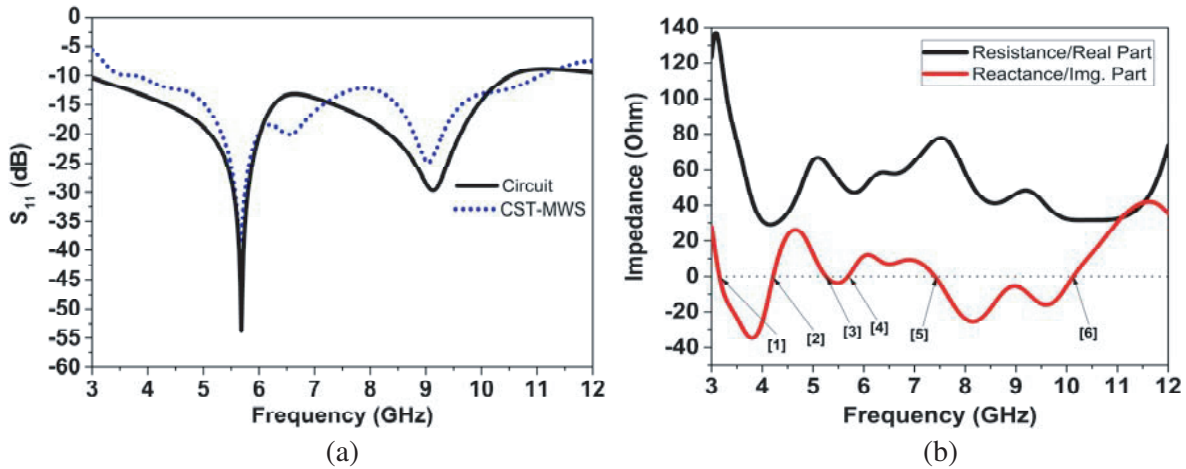


Figure 12. Simulated results. (a) S_{11} vs frequency. (b) Impedance vs frequency.

5. FABRICATION AND MEASURED RESULTS

To validate the simulation results, the proposed geometry is fabricated using a PCB prototyping machine and measured using Rohde and Schwarz vector network analyzer (ZVB14). Figs. 13 and 14 show the fabricated printed semi-annular monopole antenna and measurement setup, respectively.

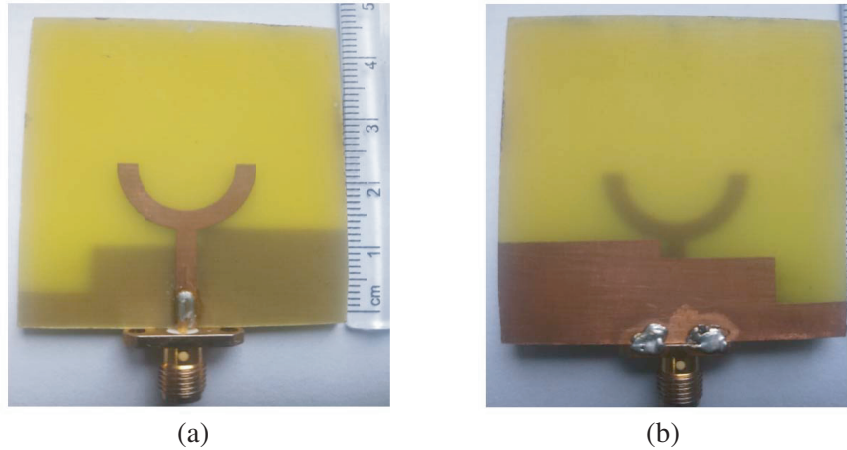


Figure 13. Fabricated printed semi-annular monopole antenna. (a) Top view. (b) Bottom view.

The simulated and measured -10 dB impedance bandwidths are 3.98–11.16 GHz (CST), 3.72–11.1 GHz (HFSS), 3.0–10.9 GHz (Circuit) and 3.22–12 GHz (Measured), respectively. Similarly, simulated and measured 3-dB AR bandwidths are 7.47–9.76 GHz (CST), 7.57–9.79 GHz (HFSS) and 7.58–9.79 GHz (Measured), respectively, as shown in Fig. 15(a). The peak realized gain and antenna efficiency are nearly about 4.32 dB at 7.61 GHz and 82% at 4.83 GHz frequency as shown in Fig. 15(b). The far-field radiation patterns in x - z and y - z planes of the designed antenna at 7.9 and 9.3 GHz are presented in Fig. 16.

It is the other method [26] to identify the polarization waves instead of electric field distributions at different phases. From the radiation pattern, it is noticed that RHCP has stronger electric fields than LHCP in broadside radiation by more than 18 dB in x - z and y - z planes at 7.9 and 9.3 GHz, respectively.

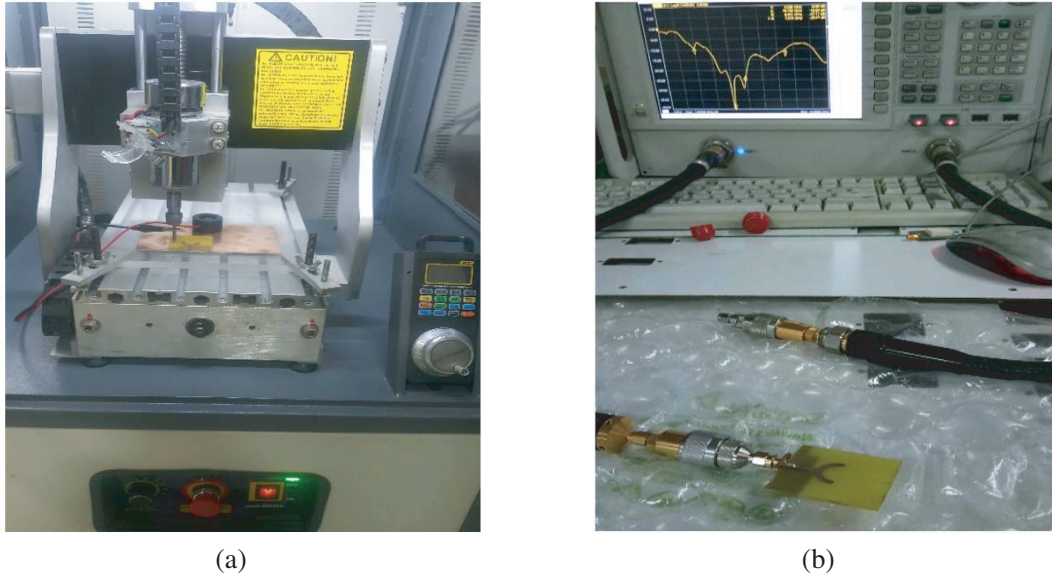


Figure 14. Fabrication and measurement setup. (a) PCB prototyping machine. (b) Vector network analyzer (VNA).

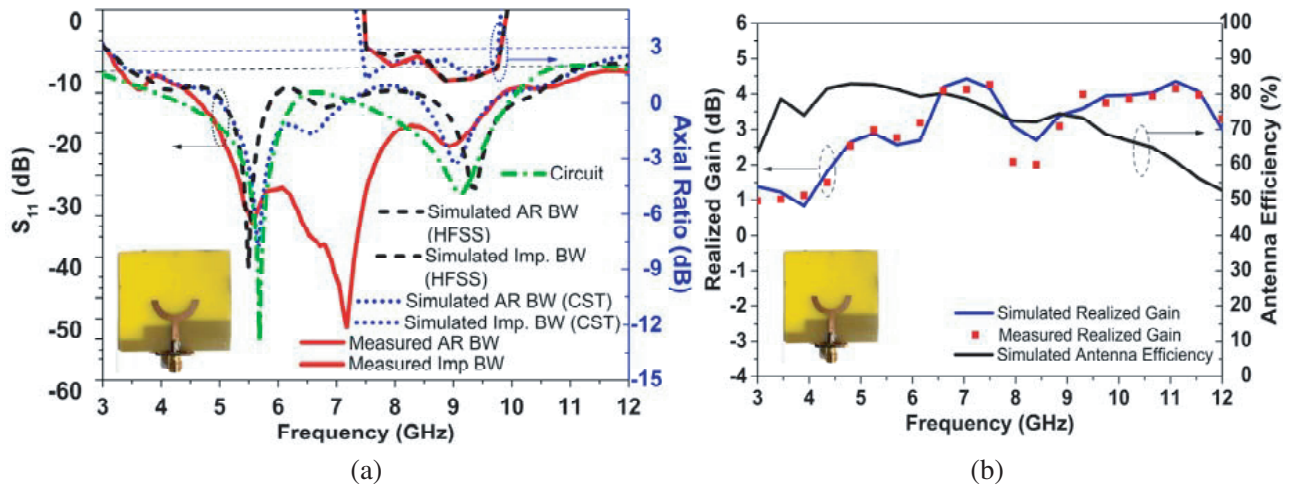


Figure 15. Compared results. (a) S_{11} & AR characteristics. (b) Realized gain & Antenna efficiency characteristics.

Therefore, the designed monopole antenna provides RHCP radiation waves. The detailed comparison of existing literatures with the proposed antenna is compared in Table 3.

6. TIME DOMAIN PERFORMANCE

In this section, the time-domain analysis of the proposed antenna is investigated. It describes the behavior of the proposed antenna with Tx/Rx a signal in the time domain. To perform this analysis, the antenna arrangements for both cases are shown in Fig. 17.

The analysis was carried out using CST-MWS solver. The plot of a Gaussian pulse source having bandwidth 3–12 GHz is used to excite the Tx antenna, and the received pulses for both the arrangements are shown in Fig. 18(a). It is observed from the graph that the received pulse is very much correlated

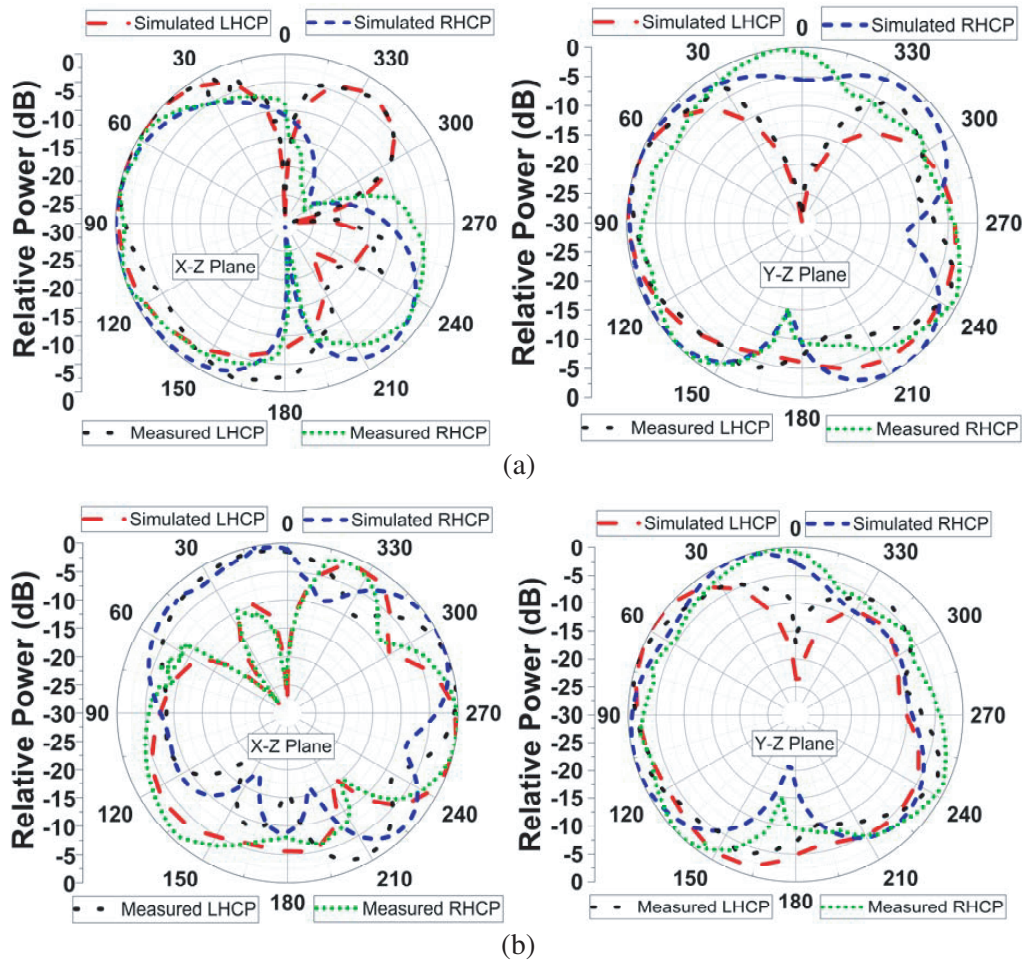


Figure 16. Radiation patterns of the proposed antenna in *X-Z* plane and *Y-Z* plane at 7.9 GHz and 9.3 GHz.

Table 3. Comparison of existing literature with proposed structure.

Ref.	CP Tech.	Imp. BW (GHz)	AR BW (GHz)	Gain (dBi)	Math. Modelling	Equivalent Circuit
[12]	Y-Shaped	2.25–2.35	2.24–2.35	2.9	No	No
[13]	Monopole with Slots	1.8–4.5	2.25–3.75	2.5	No	No
[14]	Monopole with Slots	4.06–10.02	5.91–8.55	2.9	No	No
[15]	G-Shaped & C-Shaped monopole	3.92–7.52	4.28–7.44	~ 3.5	No	No
[PS]	Monopole with Slots	3.22–12.0	7.58–9.79	4.3	Yes	Yes

~ Tech.: Techniques, Imp.: Impedance, BW: Bandwidth, Math.: Mathematical

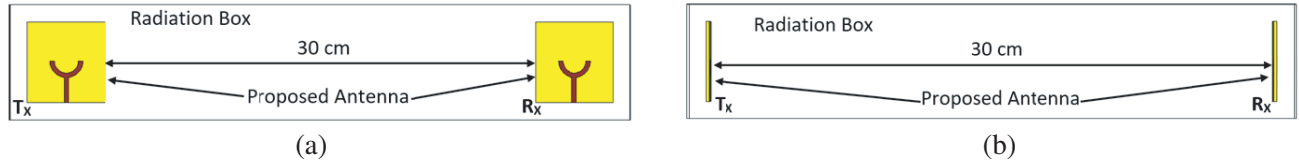


Figure 17. T-D analysis. (a) Side-By-Side characteristics. (b) Face-To-Face characteristics.

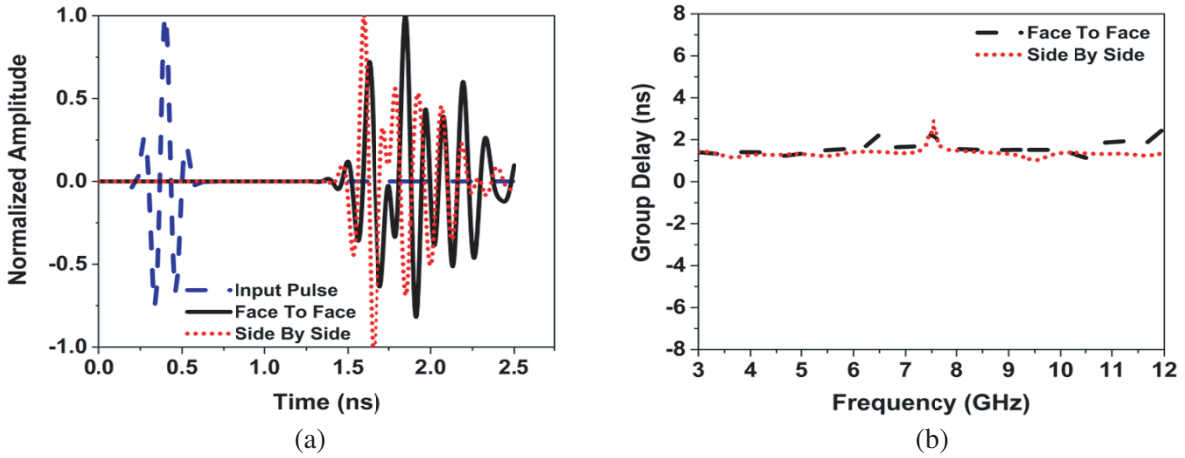


Figure 18. Output responses of T-D analysis. (a) Normalized amplitude characteristics. (b) Group delay characteristics.

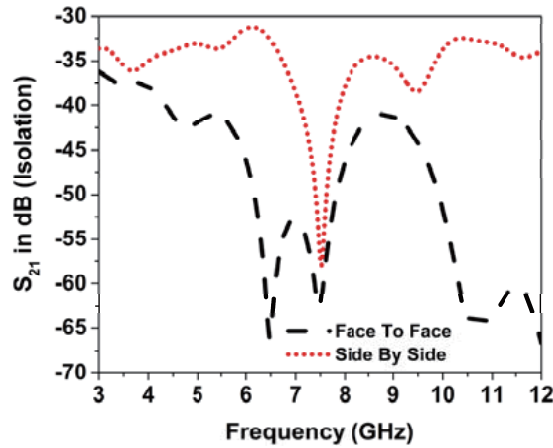


Figure 19. Time-domain analysis of S_{21} in dB (Isolation) characteristics.

with the input pulse. Group delay can be defined as the *-ve* rate of change of transfer function w.r.t. frequency. It is used to realize the pulse distortion and signal transition time between transmitted and received signals. Fig. 18(b) shows the group delay vs frequency for Face-To-Face and Side-By-Side arrangements. From Fig. 19, it is observed that the isolation is more than -30 dB for both the arrangements [27, 28]. Fig. 20 presents that the phase variation is nearly linear within the operating frequency band.

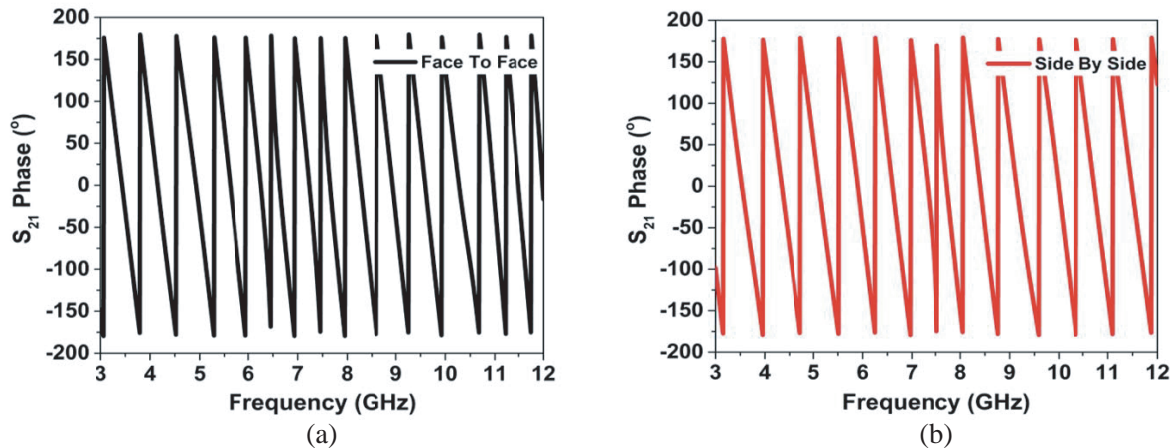


Figure 20. Time-domain analysis of S_{21} phase vs frequency. (a) Face-To-Face characteristics. (b) Side-By-Side characteristics.

7. CONCLUSION

In this paper, a circularly polarized printed semi-annular monopole antenna with broadband characteristics is proposed and investigated. An asymmetric stair-shaped partial ground plane is used to transform LP into CP with an enhancement of the impedance bandwidth. To validate CP mechanism, different methodologies like surface current distribution and electric field distribution along with mathematical modeling are analyzed and reported. Further, an equivalent circuit model of proposed antenna is developed using Foster canonical forms that consists of series inductor and capacitor with series of parallel R-L-C tank circuit. The proposed antenna provides 3.22–12.0 GHz and 7.58–9.79 GHz of measured -10 dB impedance bandwidth and 3-dB AR bandwidth, respectively. The peak realized gain and antenna efficiency are nearly 4.32 dB and 82% at 7.61 GHz and 4.83 GHz, respectively. The normalized radiation pattern is nearly omnidirectional over the operating frequency range. In addition, time domain analysis is performed for both the arrangements of the proposed structure. This proposed antenna can be a suitable candidate for C-band (4–8 GHz) and X-band (8–12 GHz) applications.

REFERENCES

1. Liang, J., C. C. Chiau, X. Chen, and C. G. Parini, "Study of a printed circular monopole antenna for UWB systems," *IEEE Trans. Antennas and Propag.*, Vol. 53, No. 11, 3500–3504, 2005.
2. Teng, P. L. and K. L. Wong, "Planar monopole folded into a compact structure for very low profile multiband mobile phone antenna," *Microwave and Optical Technology Letters*, Vol. 33, No. 1, 22–25, 2002.
3. Tiwari, R. N., P. Singh, and B. K. Kanaujia, "A modified microstrip line fed compact UWB antenna for WiMAX/ISM/WLAN and wireless communications," *Int. J. Electron. Commun. (AEU)*, Vol. 104, 58–65, 2019.
4. Manohar, M., R. S. Kshetrimayum, and A. K. Gogoi, "Printed monopole antenna with tapered feed line, feed region and patch for super wideband applications," *IET Microwaves Antenna Propag.*, Vol. 8, No. 1, 39–45, 2014.
5. Deng, C., Y. J. Xie, and P. Li, "CPW-fed planar printed monopole antenna with impedance bandwidth enhanced," *IEEE Antenna Wireless Propag. Lett.*, Vol. 8, 1394–1397, 2009.
6. Foudazi, A., H. S. Hassani, and S. M. Nezhad, "Small UWB planar monopole with added GPS/GSM/WLAN bands," *IEEE Trans. Antennas and Propag.*, Vol. 60, No. 6, 2987–2992, 2012.

7. Jiang, X., S. Li, and G. Su, "Broadband planar antenna with parasitic radiator," *Electron. Lett.*, Vol. 39, No. 23, 1626–1627, 2003.
8. Ammann, M. J. and Z. N. Chen, "A wideband shorted planar monopole with bevel," *IEEE Trans. Antennas Propag.*, Vol. 51, No. 4, 901–903, 2003.
9. Ding, K., C. Gao, Y. Wu, D. Qu, and B. Zhang, "A broadband circularly polarized printed monopole antenna with parasitic strips," *IEEE Antennas Wireless Propag. Lett.*, Vol. 16, 2509–2512, 2017.
10. Saini, R. K., S. Dwari, and M. K. Mandal, "CPW-fed dual-band sense circularly polarized monopole antenna," *IEEE Antennas Wireless Propag. Lett.*, Vol. 16, 2497–2500, 2017.
11. Chandu, D. S. and S. S. Karthikeyan, "A novel broadband dual circularly polarized microstrip-fed monopole antenna," *IEEE Trans. Antennas and Propag.*, Vol. 65, No. 3, 1410–1415, 2017.
12. Ghobadi, A. and M. Dehmollaian, "A printed circularly polarized Y-shaped monopole antenna," *IEEE Antennas Wireless Propag. Lett.*, Vol. 11, 22–25, 2011.
13. Zhou, S. W., P. H. Li, Y. Wang, and Z. Q. Liu, "A CPW-fed broadband circularly polarized regular-hexagonal slot antenna with L-shape monopole," *IEEE Antennas Wireless Propag. Lett.*, Vol. 10, 1182–1185, 2011.
14. Chen, B., Y. C. Jiao, F. C. Ren, and L. Zhang, "Broadband monopole antenna with wideband circular polarization," *Progress In Electromagnetics Research Letters*, Vol. 32, 19–28, 2012.
15. Midya, M., S. Bhattacharjee, and M. Mitra, "Broadband circularly polarized planar monopole antenna with G-shaped parasitic strip," *IEEE Antennas Wireless Propag. Lett.*, Vol. 18, No. 4, 581–585, 2019.
16. Mishra, S. K., R. K. Gupta, A. Vaidya, and J. Mukherjee, "A compact dual-band fork-shaped monopole antenna for bluetooth and UWB applications," *IEEE Antennas Wireless Propag. Lett.*, Vol. 10, 627–630, 2011.
17. Sharma, A., G. Das, and R. K. Gangwar, "Composite antenna for ultrawide bandwidth applications: Exploring conceptual design strategies and analysis," *IEEE Antennas Propag. Magazine*, Vol. 60, No. 3, 57–65, 2018.
18. Ellis, M. S., Z. Zhao, J. Wu, X. Ding, Z. Nie, and Q.-H. Hiu, "A novel simple and compact microstrip-fed circularly polarized wide slot antenna with wide axial ratio bandwidth for C-band applications," *IEEE Trans. Antenna and Propag.*, Vol. 64, No. 4, 1552–1555, 2016.
19. Jhajharia, T., V. Tiwari, D. Bhatnagar, D. Yadav, and S. Rawat, "A dual-band CP dual-orthogonal arms monopole antenna with slanting edge DGS for C-band wireless applications," *AEU — International Journal Electronics and Communication*, Vol. 84, 251–257, 2018.
20. Balanis, C. A., *Antenna Theory: Analysis and Design*, Wiley Interscience, 2009.
21. Meher, P. R., B. R. Behera, S. K. Mishra, and A. A. Althuwayb, "Design and analysis of a compact circularly polarized DRA for off-body communications," *AEU — International Journal Electronics and Communication*, Vol. 138, 7 pages, 2021.
22. Meher, P. R., B. R. Behera, and S. K. Mishra, "A compact circularly polarized cubic DRA with unit-step feed for Bluetooth/ISM/Wi-Fi/Wi-MAX applications," *AEU — International Journal of Electronics and Communications*, Vol. 128, 1–8, 2020.
23. Meher, P. R., B. R. Behera, and S. K. Mishra, "A chronological review of circularly polarized dielectric resonator antenna: Design and developments," *International Journal of RF and Microwave Computer-Aided Engineering*, 1–23, 2021.
24. Lu, Y., Y. Huang, H. T. Chattha, and P. Cao, "Reducing ground plane effects on UWB monopole antennas," *IEEE Antennas and Wireless Propagation Letters*, Vol. 10, 147–150, 2011.
25. Wang, S., A. Niknejad, and R. Brodersen, "Circuit modelling methodology for UWB omnidirectional small antennas," *IEEE Journal on Selected Areas in Communications*, Vol. 24, 871–877, 2006.
26. Kumar, R., N. Nasimuddin, and R. K. Chaudhary, "A new dual C-shaped rectangular dielectric resonator based antenna for broadband circularly polarized radiation," *International Journal of RF and Microwave Computer-Aided Engineering*, Vol. 29, 1–12, 2018.

27. Singhal, S. and A. K. Singh, "CPW-fed hexagonal Sierpinski super wideband fractal antenna," *IET Microwaves Antenna Propag.*, 1–7, 2016.
28. Meher, P. R., B. R. Behera, and S. K. Mishra, "Broadband circularly polarized edge feed rectangular dielectric resonator antenna using effective glueless technique," *Microwave and Optical Technology Letters*, Vol. 62, No. 10, 1–9, 2020.